coatings

MDPI

Article

Wear Mechanism and Life Map Construction of Nitride Coatings on Different Substrates

Zhiyang Xu [1,*], Yi Luo [2,3] and Zhengshu Huang [4]

[1] Department of Mechanical and Electrical Engineering, Tongling Polytechnic, Tongling 244061, China
[2] Tribology Research Institute, State Key Laboratory of Traction Power, Southwest Jiaotong University, Chengdu 610031, China; yluo_swjtu@163.com
[3] Chengdu Aerospace Wanxin Sciense & Technology Co., Ltd., Chengdu 610100, China
[4] Chengdu Agile Manufacturing Engineering Co., Ltd., Chengdu 610073, China; huangzhengshu_came@163.com
* Correspondence: xzy908818128@163.com

Abstract: The sliding wear and failure behaviors of CrN and AlTiN coatings on high speed steel (HSS) and cemented carbide (WC-Co) were investigated on a reciprocating test machine under different normal forces (30–120 N). The wear mechanism was explored based on the analysis of coefficient of friction (CoF), wear and damage of coating. Then, the coating service life maps were established and the factors affecting the coating life were explored. The results indicated that the bonding strength of coatings to the WC-Co substrate were larger than those to the HSS substrate. The CoFs of CrN fluctuated during the wear process, while CoFs of AlTiN coatings were closer to those of the uncoated substrates. The wear depths of coated samples were smaller than those of uncoated substrates. The wear depths were small when the coatings worked and then increased with the number of cycles and the normal forces. For the CrN coatings, they had longer service life under smaller normal forces than under the large forces. Under small forces, an adhesion layer derived from the wear debris was formed on the coating surface to reduce the wear at the beginning of the test, after that the main failure mechanism was abrasive wear and delamination. Under large forces, the main failure mechanism was spallation. For the AlTiN coatings, the main failure mechanism was spallation on the HSS substrate; however, on the WC-Co substrate it was adhesive and abrasive wear. The coatings (CrN and AlTiN) on WC-Co had longer service life under various normal forces than on the HSS. CrN coating has the better wear-resistance than AlTiN coatings.

Keywords: nitride coatings; service life; wear; failure; normal forces

Citation: Xu, Z.; Luo, Y.; Huang, Z. Wear Mechanism and Life Map Construction of Nitride Coatings on Different Substrates. *Coatings* **2022**, *12*, 1082. https://doi.org/10.3390/coatings12081082

Academic Editor: Francesco Marra

Received: 22 June 2022
Accepted: 27 July 2022
Published: 31 July 2022

1. Introduction

HSS (high speed steel) and WC-Co (a type of cemented tungsten carbide material, which is made of hard WC particles and a cobalt binder) are the two widely used metal materials for industrial components [1–3]. HSSs have excellent toughness and fracture resistance. WC-Co has high hardness and compressive strength [4–7]. During the service of the HSS and WC-Co and components, the direct sliding contact could lead to the wear losses and damages [2,8,9]. The component should be replaced when it is seriously worn. Therefore, it is necessary to improve the service life of HSS and WC-Co components.

Coatings were deposited on the surface to mitigate the wear and damage of components, and to prolong their lives [10–12]. There are various kinds of coatings used as protective coatings, such as TiC, TiN, AlTiN, CrN and AlCrN. They are widely used in the field due to the high hardness, good chemical stability, wear-resistance, corrosion resistance and oxidation resistance [13–18]. CrN and AlTiN are three types of metal nitride hard coatings [2,9]. CrN is a kind of Cr-based coating which showed corrosion-, oxidation- and wear-resistance, specially coated on soft substrates [15,16,19–21]. AlTiN coating is a kind of TiN-based ternary coating with a high concentration of aluminum. The hardness,

oxidation- and wear-resistance were increased via the incorporation of Al into the fcc-TiN structure [22,23]. Through studying and comparing the tribological properties of the coatings on different substrate materials, the best matching between coating and substrate could be determined.

In previous works, it was found that the speed, temperature, contact medium, etc. affected the tribological properties of coatings [24–31]. Vera et al. [32] deposited TiN, CrN and WC/C coatings on different steels. The coated samples were tested on the reciprocating wear tester. The results showed that WC/C coating had a lower CoF. Compared with the coatings deposited on 8620 steel and 4140 steel, the coatings deposited on 4320 steel showed better wear-resistance. Xian et al. [33] deposited TiAlN-(TiAlN/CrAlSiN)-TiAlN multilayer coatings on ceramic, cemented carbide and HSS substrates. The wear-resistance of the coatings were studied on a ball-on-disk wear tester. It was found that the coatings deposited on cemented carbide substrates had the best wear-resistance. Łępicka et al. [34] conducted a comparative study on the surface roughness, mechanical properties, adhesion and anti-wear performance of TiN coatings deposited on 316LVM stainless steel and Ti6Al4V alloy by using a ball-on-disc microtribometer. After the coatings were worn out in the wear test, the tribofilm formed on the substrate surface would protect the substrate and the CoF would decrease until the end of the test. Zhou et al. [35] coated diamond-like carbon (DLC) on SUS304 and YT15 substrate, and the reciprocating wear tester was used to explore the coating surface evolution in the long run recycling wear. The results showed that the substrate material was an important factor affecting the adhesive, tribological properties and wear life of the coating.

The service life map is an important means to systematically study the wear and failure properties of coating. It is useful for understanding the wear mechanism of the coating and explore influential factors [36–38]. Ding et al. constructed the coating response wear maps for DLC (diamond like carbon) coatings, which could illustrate more clearly the performance of coatings under different load conditions [36].

The purpose of this study is to explore the tribological properties of the two nitride coatings (CrN and AlTiN) on two substrates (HSS and WC-Co) in order to realize better application of nitride coatings. The coating service life maps were constructed based on the comprehensive analysis of CoFs, wear depth and wear scar morphologies. The establishment of the life map could not only compare the friction and wear properties of the nitride coatings but also predicted the coating life. The factors affecting the coating life and the best working force condition will be discussed, and the results will aid in coating design and selection.

2. Experimental Details

2.1. Sample Preparation

CrN and AlTiN coatings were deposited on HSS or WC-Co (WC-Co cemented carbide, brand: YG6A) substrates. Six types of samples were prepared: (1) uncoated HSS, (2) uncoated WC-Co, (3) CrN coating on HSS, (4) CrN coating on WC-Co, (5) AlTiN coating on HSS and (6) AlTiN coating on WC-Co. The dimensions of samples were 20 mm × 10 mm × 10 mm.

An industrial cathodic arc plasma deposition system was used for coating deposition. Before the deposition, the substrates were ultrasonically cleaned and dried, then etched via the argon bombardment. A thin film (chromium film for CrN coating, and aluminum-titanium alloy film for AlTiN coating) was deposited on the substrates as an interlayer to improve the adhesion between coating and substrate [16,39]. The interlayer was deposited on the substrate for 2–3 min. After that, the CrN or AlTiN coating was deposited on the interlayer. The parameters of the deposition processes are shown in Table 1. The deposition temperature of both coatings did not exceed 400 °C, and the deposition time was 40 min.

Table 1. Deposition parameters of CrN and AlTiN coatings.

Coatings	Cathode Targets	Temperature (°C)	Current (A)	Bias (V)	Deposition Time (min)
CrN	Cr	380	120	−60	40
AlTiN	AlTi	400	160	−50	40

2.2. Coatings Characterization

The mechanical properties and roughness of the substrates and coatings are listed in Table 2. The hardness and Young's modulus of WC-Co were larger than the HSS. The roughness of HSS and WC-Co substrates was close. Compared with the roughness of the uncoated substrates, the roughness of the coatings was slightly higher but smaller than 0.2 µm. The nanoindentation hardness of the AlTiN coating was larger than CrN coating, but the Young's modulus of the CrN coating was larger than AlTiN coating [40].

Table 2. Mechanical properties and roughness of substrates and coatings.

Sample	Hardness ($HV_{0.5}$)	Nanoindentation Hardness (GPa)	Young's Modulus (GPa)	Poisson's Ratio	Roughness Ra (µm)
HSS substrate	680 ± 25	-	210	0.27	0.095 ± 0.015
WC-Co substrate	1300 ± 20	-	510	0.22	0.07 ± 0.025
CrN coating	-	23.4 ± 5.5	473.2 ± 90	0.25	0.15 ± 0.03
AlTiN coating	-	31.8 ± 6.6	359.9 ± 40	0.25	0.10 ± 0.05

The scanning electron microscope (SEM) images of surfaces and cross-sections of the coated samples are shown in Figure 1. Both the CrN and AlTiN coatings had the similar thickness (around 3 µm) on the HSS and WC-Co. There were a few holes, particles and droplets on the coatings which did not affect the natural test and application of the coating.

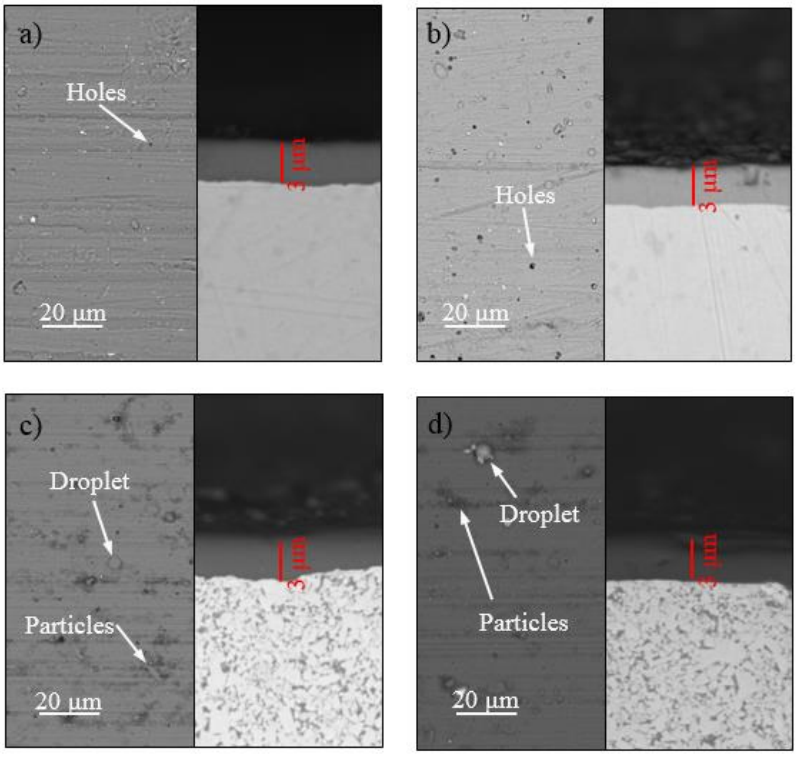

Figure 1. SEM images of the surfaces and cross-sections of coated samples: (**a**) CrN on HSS; (**b**) AlTiN on HSS; (**c**) CrN on WC-Co; (**d**) AlTiN on WC-Co.

The result of energy dispersive spectroscopy (EDS) analysis on the substrates and coatings is shown in Table 3. HSS was mainly composed of C, Cr and Fe. WC-Co was mainly composed of C, W and Co. The CrN coating mainly contained N, Cr. The AlTiN coating mainly contained N, Ti and Al. Note that, the EDS are not good at detecting the light elements because too less signal could be received. But the values could be used to compare the contents of a certain element among different materials.

Table 3. Chemical element compositions of substrates and coatings detected via EDS.

Elements (Wt %)	C	N	O	Al	Ti	Cr	Fe	Co	W
HSS	12.92					7.26	79.82		
WC-Co	15.94		1.68					8.06	74.32
CrN coating	2.78	68.28				28.94			
AlTiN coating	2.13	41.59		27.47	28.81				

The bonding strengths of the coatings on the substrates were measured via the scratch tests, which were conducted on a scratch tester (FISCHERSCOPE-ST200, Germany), using a diamond indenter with a radius of 200 μm. The coatings were scratched with a progressive load increasing from 0.5 N to 100 N at a constant sliding speed of 3 mm/min, and the scratch length was 3 mm. Scratch tests were repeated three times.

According to the topography, penetration depth and the acoustic emission during the scratch process, the values of critical load of the coatings falling off can be obtained, as shown in Table 4. The coatings on WC-Co substrate had higher critical loads than those on the HSS substrate. This was because the hardness and the Young' modulus of WC-Co substrate were higher than the HSS substrate and closer to those of coatings (Table 1). The critical load of CrN coating was higher than that of AlTiN coating, which was because of the lower hardness of CrN than AlTiN.

Table 4. Critical load of coated samples.

Samples	CrN Coating on HSS	CrN Coating on WC-Co	AlTiN Coating on HSS	AlTiN Coating on WC-Co
Critical load (N)	48.2 ± 5.4	92.8 ± 3.3	42.3 ± 4.4	78.0 ± 3.5

2.3. Reciprocating Wear Test Process

Reciprocating wear tests were conducted on a reciprocating sliding machine, as shown in Figure 2. A normal force was applied on the counter body (a WC-Co ball with a diameter of 6 mm; brand: YG8; Young's modulus: 510 GPa; the hardness: around 1520 HV). The force was measured via a pressure sensor. The friction force was detected via a tension/pressure sensor. Data from the sensors were recorded to calculate the real-time coefficient of friction.

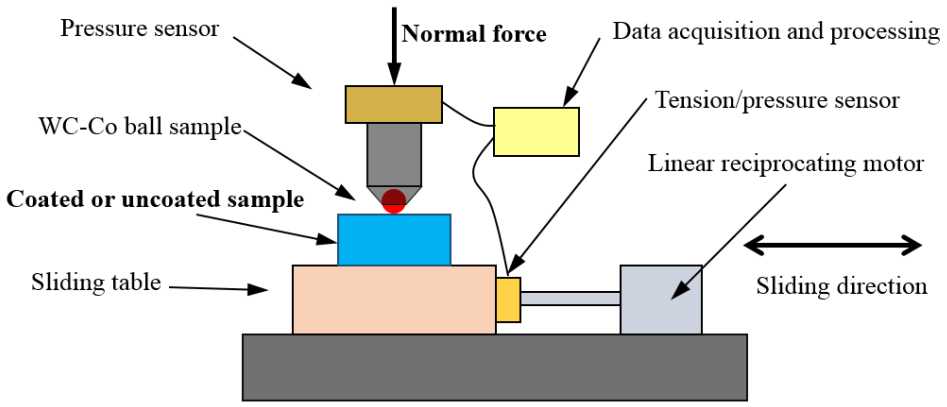

Figure 2. Schematic of the reciprocating sliding test machine.

The tests were conducted under four different normal forces (i.e., 30 N, 60 N, 90 N and 120 N). The normal forces of 30–120 N led to the initial maximum contact pressures of 2538–4029 MPa on the HSS substrate, and 3591–5700 MPa on the WC-Co substrate, without consideration of the influence of coating. To explore the life and the wear process, tests were conducted for different numbers of cycles from 100 to 50,000 cycles. The parameters of test normal forces and numbers of cycles were shown in Table 5. All tests were performed in air conditions at room temperature. The reciprocating frequency was 2 Hz and the amplitude was 2 mm.

Table 5. Test parameters.

Samples Type	Normal Force (N)	Number of Cycles
HSS, CrN on HSS, AlTiN on HSS, WC-Co, CrN on WC-Co, AlTiN on WC-Co	30, 60, 90, 120	10–50,000 (depending on the failure process of coating)

During the reciprocating sliding wear test, the CoF was recorded. After the test, the average value of the last 10 CoF points on the curve were calculated, which was taken as the final CoF value. The samples were ultrasonically cleaned. The profiles of the wear scars were measured using a profilometer (JB-6C, Shang hai, China). Five profiles perpendicular to the sliding direction were measured, evenly distributed on the wear scar. The wear depth was obtained by calculating the average of the maximum wear depth values of the five profiles. The wear scars were observed and analyzed using an optical microscopy (OM) (KEYENCEVHX-6000, Osaka, Japan), a scanning electron microscopy (SEM) (Phenom Pro-SE, Eindhoven, Netherlands) and an energy dispersive spectroscopy (EDS) (JSM-6610LV, Akishima-shi, Japan).

3. Results and Discussion

3.1. Coefficient of Friction

The CoFs as a function of cycle number on the uncoated HSS and WC-Co samples are shown in Figure 3. The stable CoF of HSS substrate was around 0.7–0.8, which was higher than the stable CoF of the WC-Co substrate (around 0.2–0.3). The normal forces had no obvious influence on the stable CoF of the uncoated samples.

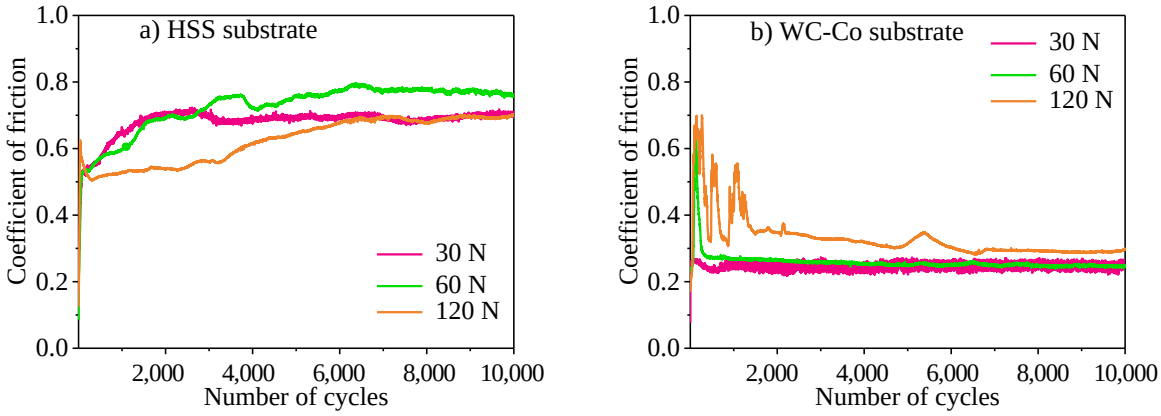

Figure 3. CoFs of uncoated samples as a function of cycle number under various normal forces: (**a**) HSS substrate; (**b**) WC-Co substrate.

Figure 4a shows the CoFs as a function of cycle number on a representative coated sample (CrN coating on HSS substrate) under different normal forces. At the beginning of the test, the CoFs were low. With the test ongoing, the CoFs increased, because the coating

was worn off. After that the CoF remained relatively high. The normal force had influence on the CoF evolution, because the normal force affected the wear and failure processes of coatings. Under the small normal forces (30 N and 60 N), CoFs increased smoothly because CrN coating was worn off gradually. Under the large normal forces (90 N and 120 N), the CoFs increased relatively sharply because the coatings were removed and failed quickly. Furthermore, the larger normal force which led to the increase of CoF occurred earlier. For example, the CoF increased after 100 cycles under 90 N while it increased after 10 cycles under 120 N (Figure 4a).

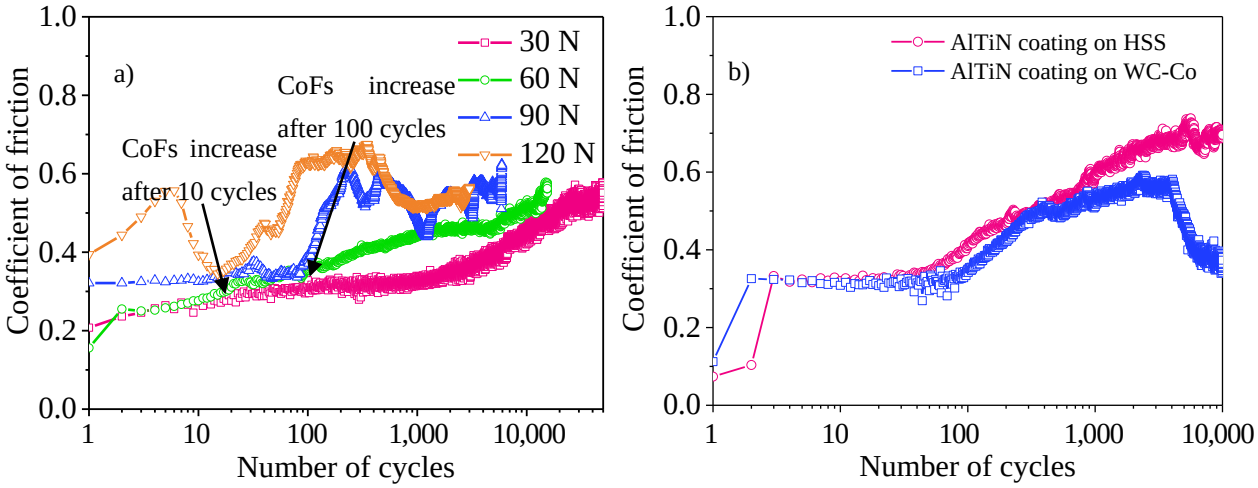

Figure 4. CoFs as a function of the number of cycles: (**a**) CrN coating on HSS substrate under different normal forces; (**b**) AlTiN coating on HSS and WC-Co substrates under 30 N normal force.

The change of CoF can help to judge the failure process of the coatings. After the coating was removed off, the CoF would be similar to that of substrates. As shown in Figure 4b, with the increase in cycles, the CoF of AlTiN coated HSS sample remained high (around 0.7–0.8, close to the CoF of uncoated HSS), the CoF of AlTiN coated WC-Co sample decreased to low values (around 0.3–0.4, close to the CoF of uncoated WC-Co).

Figure 5 shows the final CoFs of samples at the end of the tests (for example, the average values of the last 10 CoF points in Figures 3 and 4). The CoFs of HSS substrate (Figure 5a) increased with the number of cycles. The CoFs of WC-Co substrate (Figure 5b) decreased with the number of cycles. The CoFs of the CrN coated HSS substrate (Figure 5c) and the CrN coated WC-Co substrate (Figure 5d) fluctuated in the range of around 0.3–0.7, this might because the coating fell off and the third body materials formed at the contact interface. The AlTiN-coated HSS substrate (Figure 5e) had the CoFs of around 0.4–0.6 at 100 cycles. With the increase in the number of cycles, the CoF increased to the similar CoF level of HSS substrate (0.7–0.8). The CoFs of the AlTiN-coated WC-Co substrate (Figure 5f) increased first and then decreased to a similar CoF level of the WC-Co substrate (around 0.3). It was found that the CoFs of the AlTiN-coated HSS substrate (0.4–0.6) and the AlTiN-coated WC-Co substrate (0.2–0.4) were different at 100 cycles, which might be because the AlTiN coating was removed rapidly on the HSS, while it was not significantly removed on the WC-Co in the early stage.

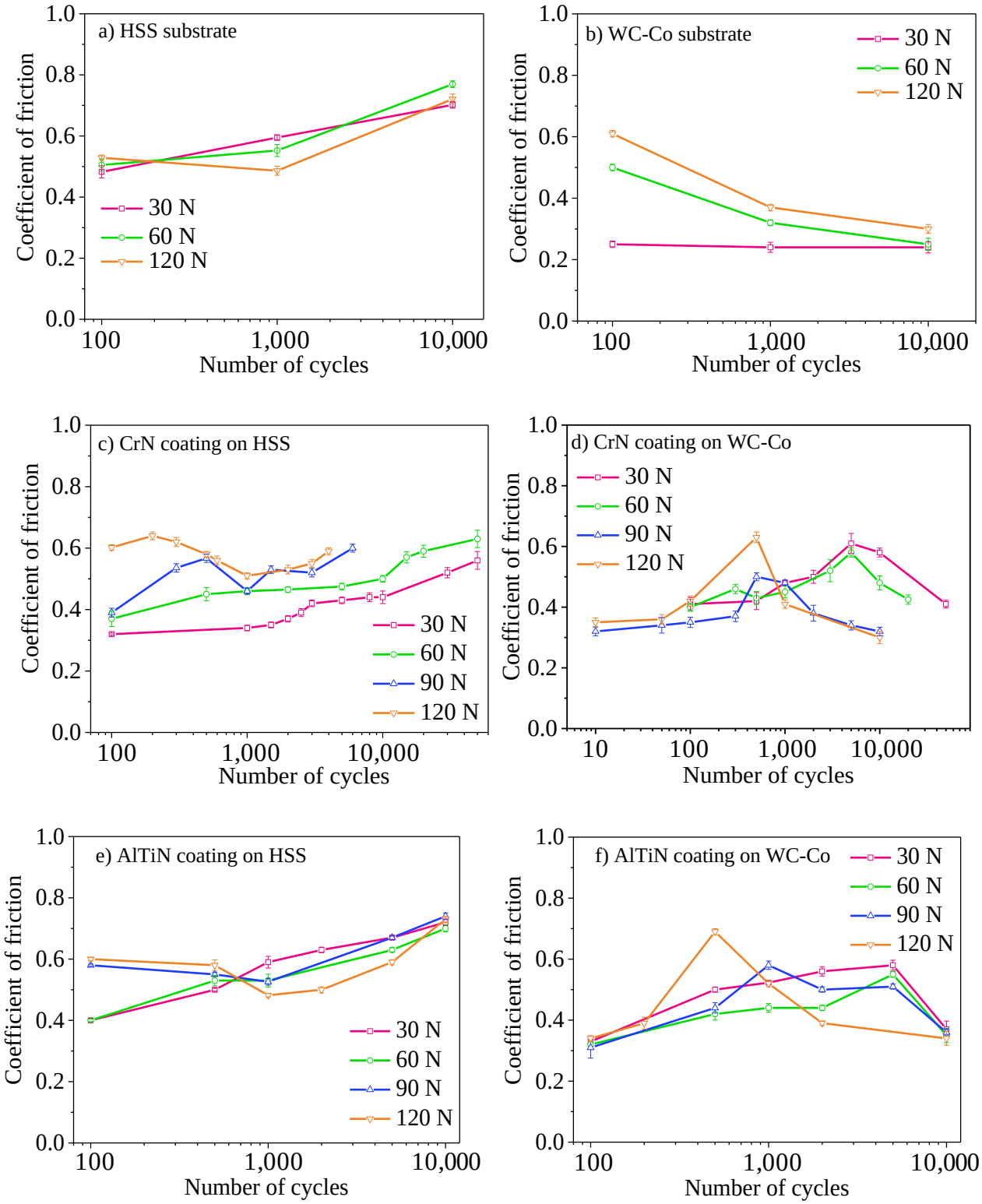

Figure 5. The final CoFs: (**a**) HSS substrate; (**b**) WC-Co substrate; (**c**) CrN coating on HSS; (**d**) CrN coating on WC-Co; (**e**) AlTiN coating on HSS; (**f**) AlTiN coating on WC-Co.

3.2. Wear Depth

Representative wear scars of coated samples (CrN coating on the HSS substrate) under different forces and their profiles are shown in Figure 6. Under the mild load condition (30 N for 1000 cycles), the coating was not removed, and the depth of the wear scar was around 2.3 μm, which was smaller than the thickness of the coating (3 μm). Thus, the coating was

not totally worn off. However, under the severe condition (120 N for 2000 cycles), the coating at the contact area was totally removed and the depth (around 16.9 μm) exceeded the coating thickness.

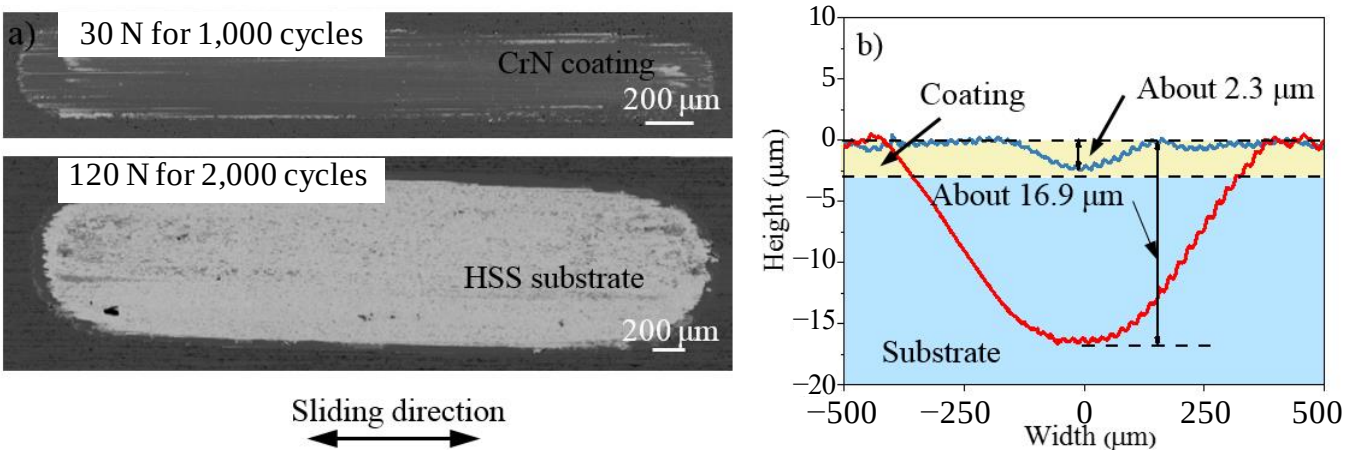

Figure 6. (**a**) SEM of wear scars and (**b**) profiles of CrN coated HSS substrate.

The wear depths of uncoated and coated samples (Figure 7) increased with the number of cycles and the normal forces. The wear depths of the coated samples (Figure 7c–f) were smaller than those of substrates (HSS and WC-Co substrate, Figure 7a,b). This means that the CrN and WC-Co coatings could improve the wear-resistance of the HSS and WC-Co substrates. The wear depth of the HSS substrate (Figure 7a) was larger than the wear depth of the WC-Co substrate (Figure 7b) because the hardness of WC-Co is higher than HSS (Table 2). Furthermore, the sharp increase in wear depth occurred earlier under the larger normal forces, which might be due to the rapid failure and removal of coatings.

In addition, the plastic deformation of the substrate could increase the depth of the profile of wear scar. The wear depth of coated samples was slightly larger than the thickness of the coating, but the coating could still exist in the contact area. The deformation and abrasive resistance of WC-Co substrate was greater than that of the HSS substrate, which led to lower wear depth of coated WC-Co samples than that of coated HSS samples.

3.3. Wear Scar Morphologies

3.3.1. HSS and WC-Co Substrates

The representative wear surface of HSS and WC-Co substrates under 120 N normal force are shown in Figure 8. For HSS substrate (Figure 8a), the wear debris had adhered to the surface after 100 cycles. After 1000 cycles, the more wear debris was adhered forming a three-body film, and cracks could be observed on the substrate. After 10,000 cycles, the adhered material was removed and some wear debris filled in the cracks to aggravate their propagation. This was also the reason why the stable CoFs of HSS substrate sample were at a high level of 0.7–0.8 (Figure 3a).

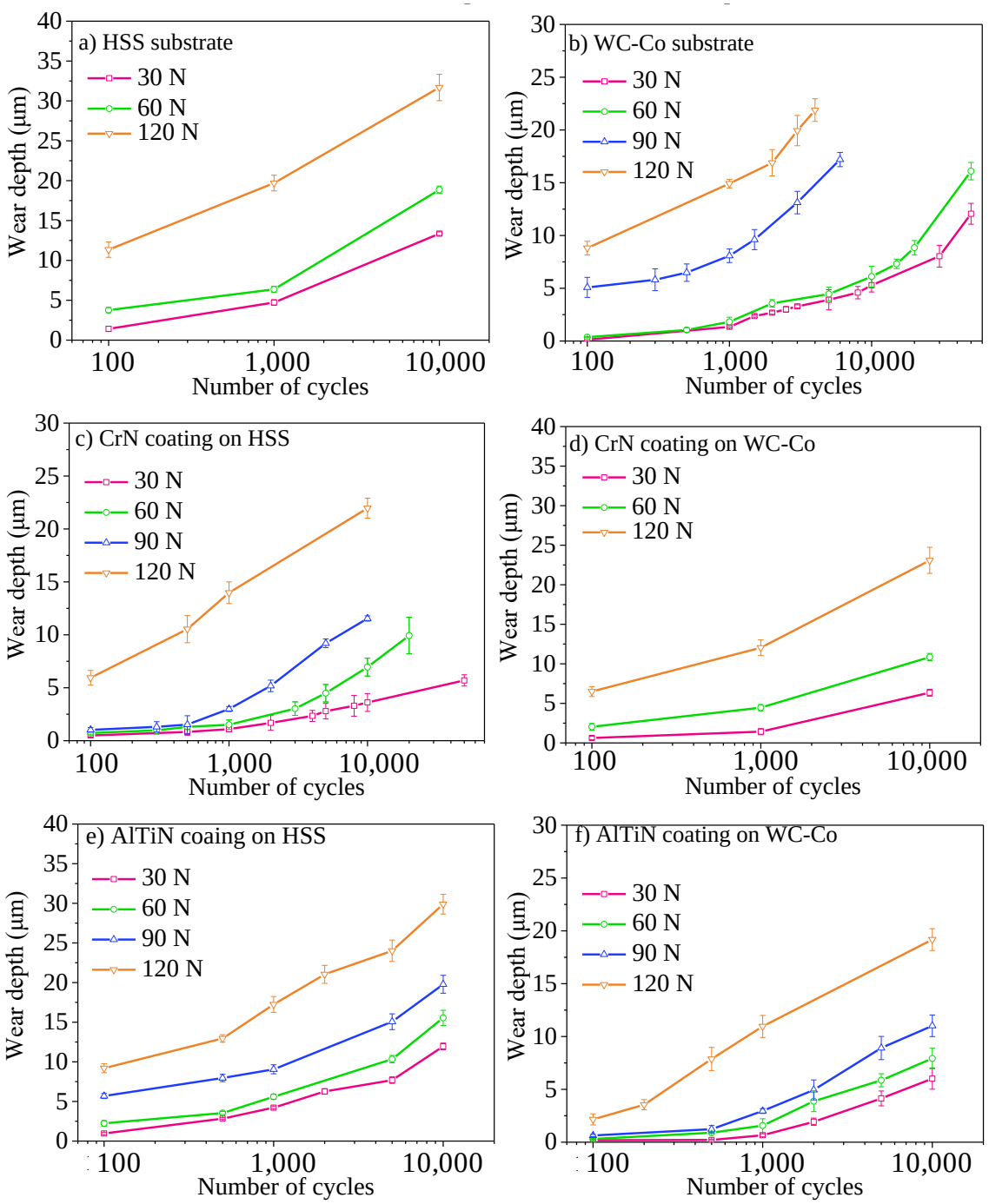

Figure 7. Wear depths: (**a**) HSS substrate; (**b**) WC-Co substrate; (**c**) CrN coating on HSS; (**d**) CrN coating on WC-Co; (**e**) AlTiN coating on HSS; (**f**) AlTiN coating on WC-Co.

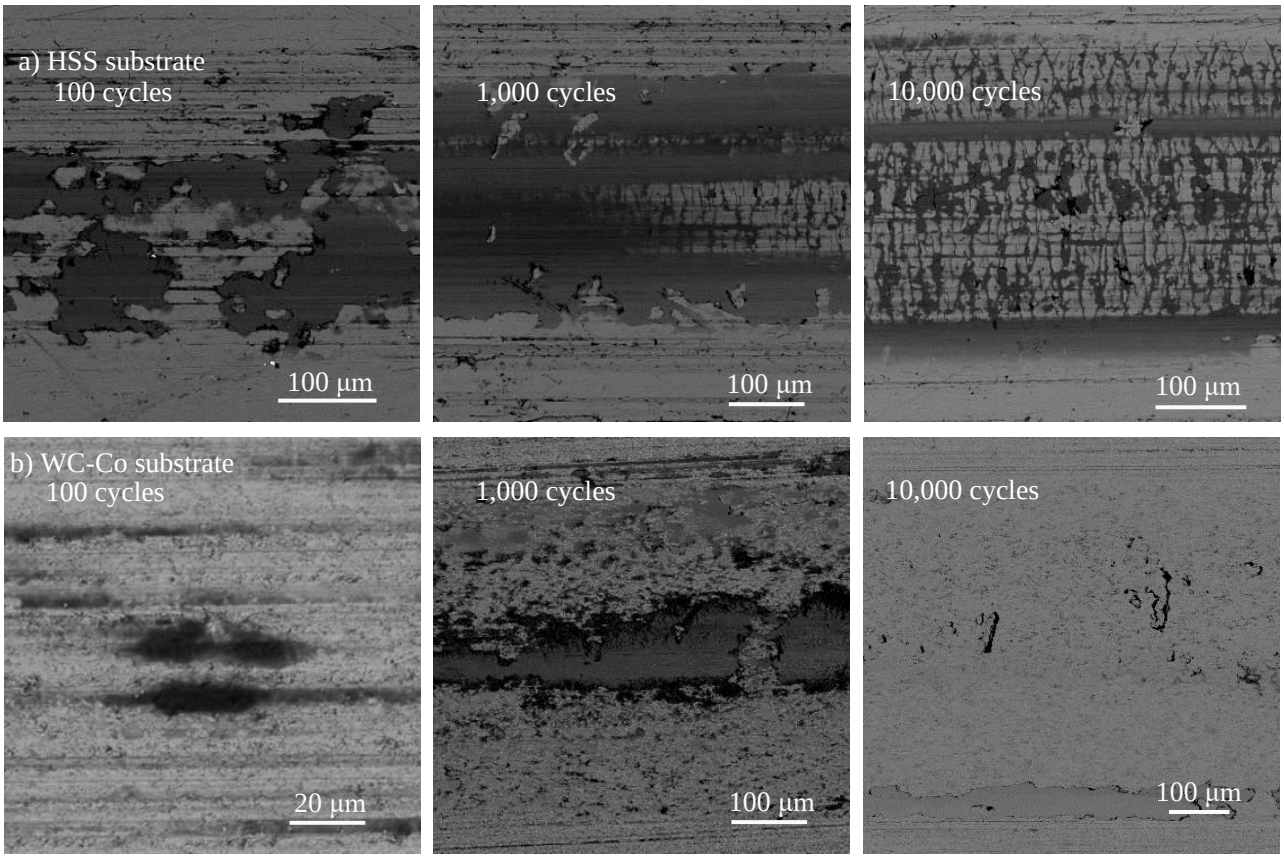

Figure 8. Wear process of uncoated samples: (**a**) HSS; (**b**) WC-Co.

For the WC-Co substrate (Figure 8b), the wear debris was also adhered to the worn surface, but when the number of cycles was increased to 10,000, the adhesive wear debris on the surface of WC-Co samples was removed and the surface became more smooth, which resulted in stable CoFs at a low level of 0.2–0.3 (Figure 3a). Because WC-Co has high hardness, it was not easy to produce initial cracks.

3.3.2. CrN Coating on HSS Substrate

Under different normal forces, the wear scar morphologies of coatings were different during the wear process (Figure 9). Under 30 N, the surface of the coating was polished without notable removal after 2000 cycles. After 5000 cycles, a thin adhesive layer was formed on the surface of the CrN coating. According to the EDS analysis (Table 6), the point A in the Figure 9 was mainly composed of C, W, Cr, Fe, N, Co and O elements. C, W and Co elements were derived from the adhesive layer (i.e., the wear debris of the counter body). The EDS analysis of the adhesion layer detected Cr and N, but this did not prove that the adhesion layer composition included Cr and N, because the EDS could detect a certain depth of material (including the adhesive layer and the coating). The surface of counter body was clean without adhesive materials (Figure 10). Moreover, the presence of the O element means that oxidation occurred during the formation of the adhesive layer. After running for 8000 cycles, the adhesive layer had been spalled due to wear. After 50,000 cycles, the adhesive layer had been totally removed, but the coating still existed in a good condition on the substrate. In summary, the CrN coating on HSS worked well even after 50,000 cycles under 30 N.

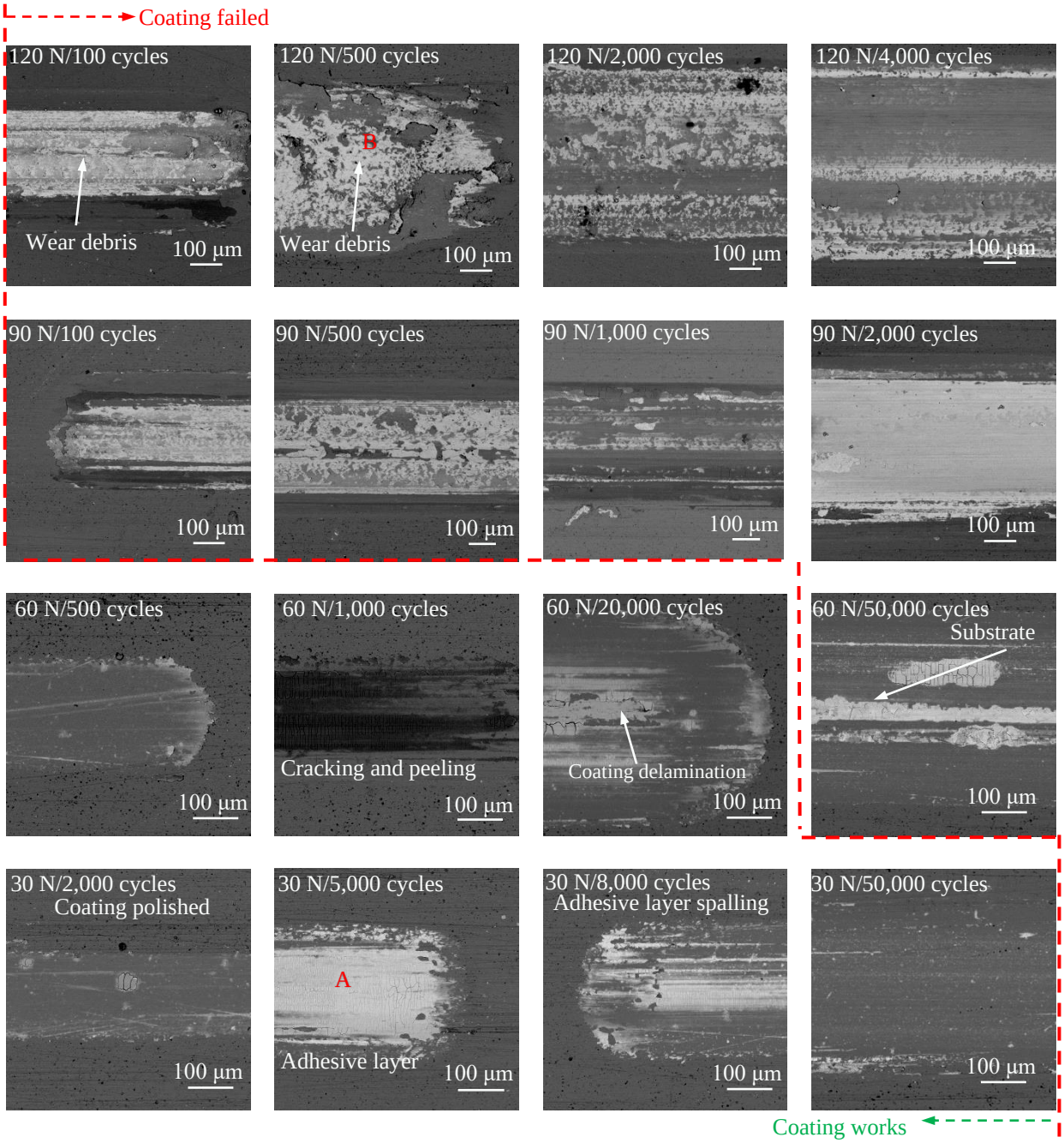

Figure 9. Wear and failure process of CrN-coated HSS under different normal forces.

Table 6. EDS analysis of the points A and B in Figure 9.

Elements (Wt.%)	C	N	O	Cr	Fe	Co	W
A	5.81	22.98	4.58	64.70	0.38	0.24	1.31
B	8.36	12.29	4.54	16.30	56.31	-	1.71

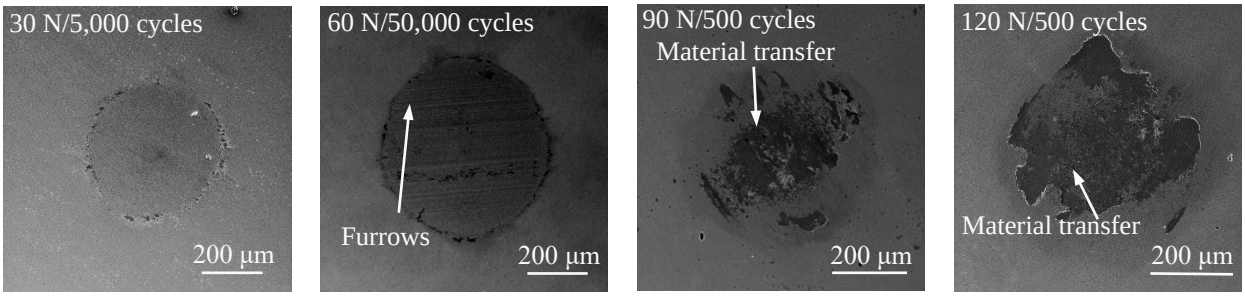

Figure 10. Wear scar of the counterbody against the CrN-coated HSS substrate under different condition.

Under 60 N, the wear degree was higher than that under 30 N. The cracking and peeling of adhesive layer occurred after 1000 cycles. A small part of coating delaminated at the middle of the contact area after 20,000 cycles. After 50,000 cycles, the middle part of coating was removed, and there were furrows on the surface of the counter body (Figure 10).

Under 90 N and 120 N, even after 100 cycles, the coating was completely spalled. It might because the cohesive failure of the coating occurred under large normal forces. Some wear debris had been transferred to the exposed HSS substrate and the counter body (Figure 10) after 500 cycles. According to the EDS analysis (Table 6) of the B point in Figure 8, this wear surface consisted of C, W (from the counter body), Fe (from the HSS substrate), N and Cr (from coating debris). It means that although the coating had completely spalled, the components of the coating existed in the wear debris. After that, the wear debris formed a tribological film on the bare substrate surface under the sliding of the ball. This is also the reason why the CoFs do not reach the stable CoF of HSS substrate (0.7–0.8) after coating failed (Figure 5c). After 4000 cycles under 120N normal force, no cracks were found on the exposed HSS substrate surface, indicating that the film formed by wear debris containing CrN components also had a protective effect on the substrate.

3.3.3. CrN Coating on WC-Co Substrate

The CrN coating on WC-Co displayed a similar wear process as that of HSS but the force-resistance ability was better, due to the better bonding strength (Table 4). The CrN coating on the HSS under 90 N were removed and failed fast (less than 100 cycles), but the CrN coating on the WC-Co was still worked for longer than 2000 cycles and failed after 5000 cycles (Figure 11). Similarly, the wear degree of counter body was similar. The material more easily adhered to the counter body after the coating failed and removed (Figure 12)

In summary, the CrN coating had good resistance to adhesive wear on both substrates under small forces (30 N and 60 N). Meanwhile, the wear degree was mild (Figure 7c,d), due to a protective adhesive layer formed on the CrN coating surface to reduce the wear of the coating. The main failure mechanism of the CrN coating under small normal force were abrasive wear and delamination. On the other hand, the wear of coating was severe under the large forces (90 N and 120 N). The main failure mechanism of the CrN coating was spallation.

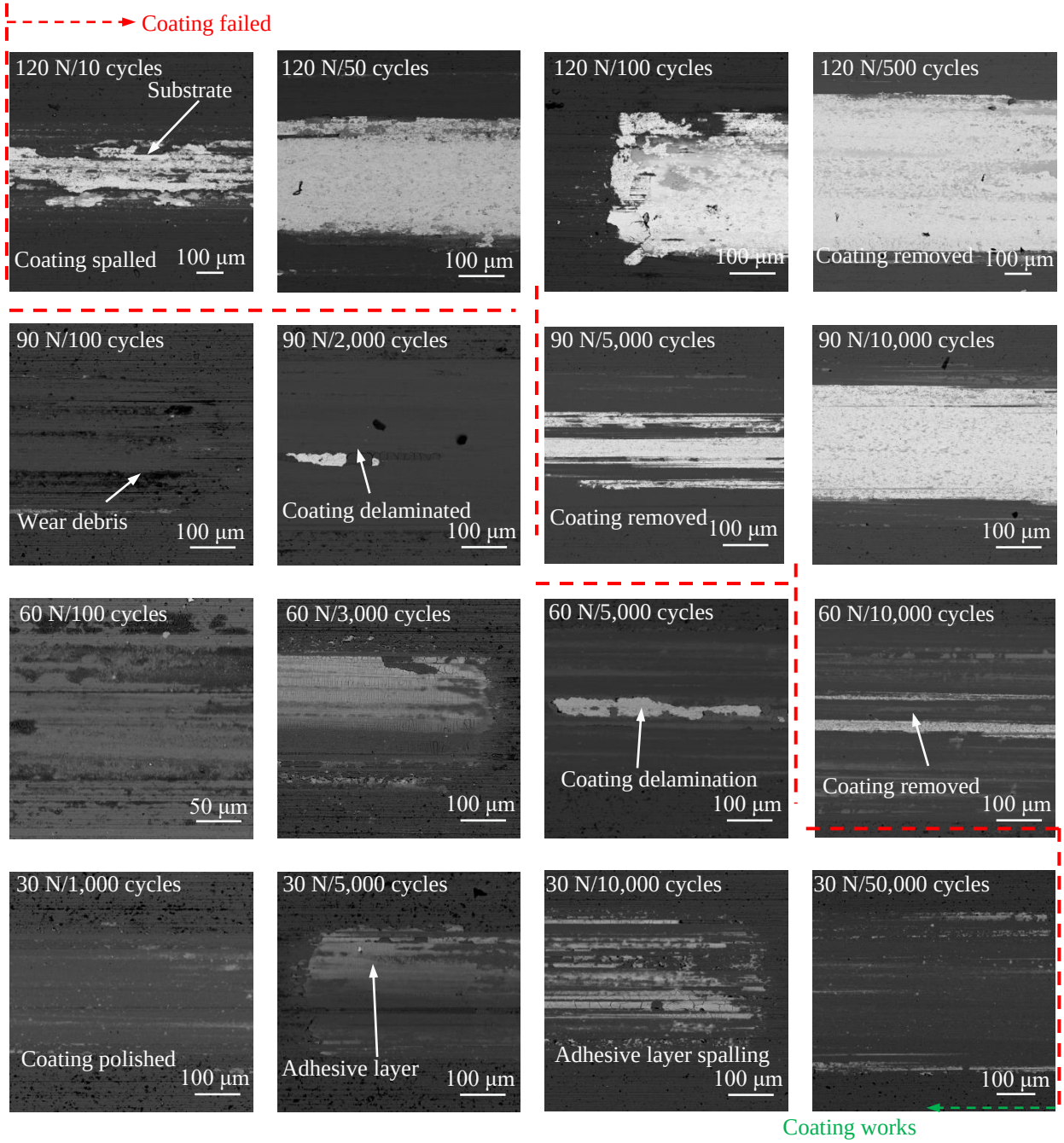

Figure 11. Wear and failure process of CrN coated WC-Co substrate under different normal forces.

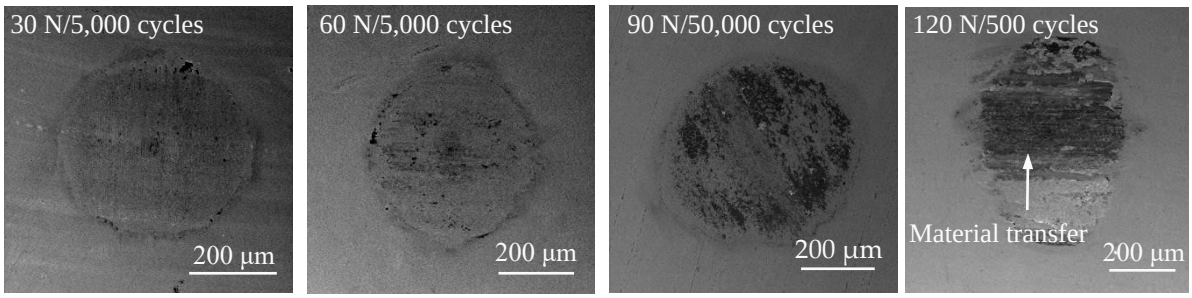

Figure 12. Wear scar of the counterbody against the CrN-coated WC-Co substrate under different condition.

3.3.4. AlTiN Coating on HSS Substrate

The wear process of the AlTiN coating on HSS is shown in Figure 13. The coating very easily failed under any load condition. Under 30 N, after 100 cycles, most of the coating still existed on the surface and only a small part of coating was spalled. After 500 cycles, the coating was completely removed. Under larger forces (60–120 N), the AlTiN coatings on the HSS substrate were totally removed very quickly ($\leq$100 cycles), because the deformation of the HSS substrate accelerated the spallation of the AlTiN coating. The substrate material type played an important role in the wear and failure behaviors of AlTiN coating [9,34,41]. The AlTiN coating had poor binding properties to the HSS substrate compared with CrN coating, because the hardness difference between the AlTiN coating and HSS was large (Table 4), thus the AlTiN coated on HSS had poor capacity to withstand the normal force and friction force. Moreover, under different forces, the wear debris material was formed the counter body (Figure 14), as previously observed after the CrN coating failure.

3.3.5. AlTiN Coating on WC-Co Substrate

Figure 15 shows the wear scars of the AlTiN coating on WC-Co substrate. There was no adhesion layer formed on the AlTiN coating surface. While the coating surface was polished, the particles were observed on the worn surface in the early wear progress, which might aggravate the wear. Furthermore, the material transfer and mild oxidation occurred on the counter body, as shown in Figure 16. Therefore, the CoF increases first (Figure 5f) in the wear process, which was caused by the three body wear and adhesive wear.

In summary, the AlTiN coating on WC-Co (Figure 15) had a higher capacity to withstand the normal force than on the HSS substrate (Figure 13), because the bonding strength of AlTiN coating was better with WC-Co than with HSS. This also resulted in that the AlTiN coating had a completely different failure mechanism. The main failure mechanism of the AlTiN-coating on HSS was spallation. However, the main failure mechanism of the AlTiN-coating on WC-Co was the abrasive and adhesive wear.

In addition, comparing the CrN-coated WC-Co to the AlTiN-coated WC-Co, the latter has poor coating–substrate bonding strength (Table 4) but it shows the better resistant to force. Specifically, CrN coated on WC-Co could not resist the force above 90 N, while AlTiN coated on WC-Co failed under 120 N and after 200 cycles. This may be due to the lower Young's modulus of the AlTiN coating than CrN, which made AlTiN coating a better toughness. The AlTiN coated on WC-Co had worse wear-resistance under small forces but better spalling and delamination resistance under large forces.

3.4. Coating Service Life Mapping

The coatings service life map was established to better explore the service law of the coatings, helping further analysis the factors affecting the wear service life of the coatings. In addition, the service life map provides ideas for better guiding the application of the coating and can be used to predict the coating life under specific service conditions. It can also be used to estimate the best working load that the coating can bear.

Utilizing the comprehensive analysis of CoFs, wear depth and wear scar morphologies [36,42] can determine whether the coating has failed. Furthermore, the maps of coating service life under different normal forces could be drawn, as shown in Figure 17. The dotted curves between the coating working area and the failed area could be regarded as the service life of coatings. The wear progress of coatings could be divided into two stages, based on whether the coating failed or not: (1) the coating working stage, where the number of cycles was smaller than the service life. CoFs and wear depths were small (Figures 5 and 7) and the coating was not or only partially removed; and (2) the coating failed the stage where the number of cycles was larger than the service life. CoFs tended to approach the CoFs of the substrates (Figure 5), wear depths were high and exceeded the thickness of coatings (Figure 7) and the coating had been almost totally removed.

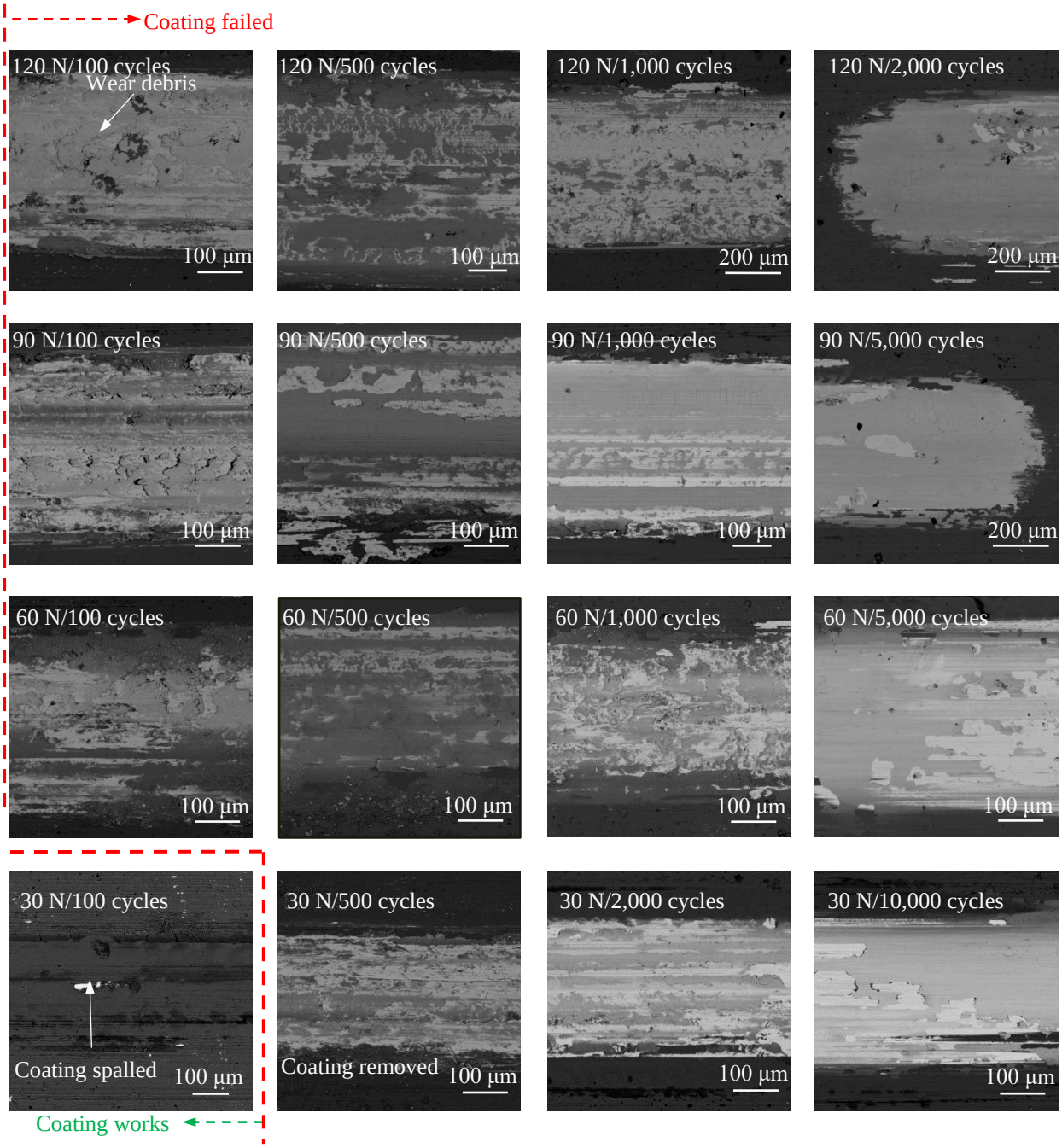

Figure 13. Wear and failure process of AlTiN coated HSS substrate under different normal forces.

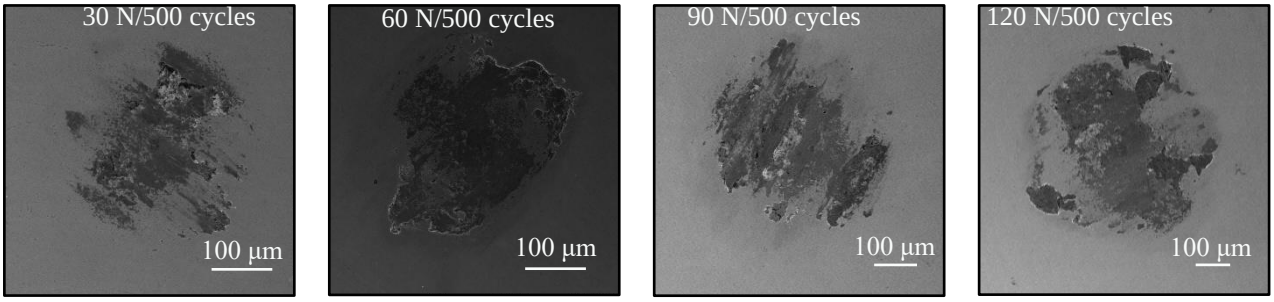

Figure 14. Wear scar of the counterbody against the AlTiN-coated HSS substrate under different conditions.

The nitride coatings studied in the present work could be applied in various practical applications, such as cutting tools, molds and bearings. The results have shown that coatings deposited on different substrate materials exhibit different friction and wear properties. Therefore, ensuring that coatings are deposited on suitable substrate materials is a prerequisite for designing coatings and an important means to improving the life of the coating system.

Through the comparison of service life maps, it can be found that the normal force, wear failure mechanism of coatings, deformation-resistance of substrates and bonding strength between the substrates are important factors affecting the service life of coated samples.

The greater normal forces, i.e., the greater Hertzian contact pressures, resulted in the greater friction forces between the ball and flat contact surface and further aggravated the wear damage degree of the samples. Therefore, the greater normal force led to the less coating life. Under 30 N and 60 N, the CrN coating shows a longer service life than AlTiN on the two substrate materials with large differences in hardness and Young's modulus. On the one hand, CrN has better bonding properties than AlTiN (Table 4). The main failure mechanism of CrN was abrasive wear, and CrN would adsorb the third body material on the coating surface during the wear process to form an adhesive layer, which could slow down the adhesive wear and abrasive wear of the coating and improve the service life of CrN. The formation of the adhesive layer seriously affected the wear-resistance and service life of the coating. It was also found that the CrN coating on HSS (Figure 17a) had longer service life than CrN coating on WC-Co (Figure 17b) under 60 N normal force, but CrN on HSS had lower bonding performance than CrN on WC-Co (Table 4), which might be caused by the instability of adhesive layer performance.

If the normal force was larger than 90 N, the service life of CrN coating on HSS was less than 100 cycles (Figure 17a). However, for the CrN coating on the WC-Co substrate, which had better bonding strength (Table 4) and deformation-resistance due to the higher hardness and Young's modulus (Table 2), the service life of the coating was about 2000–5000 cycles (Figure 17b). CrN, under 120 N normal force, could cause serious spalling failure, thus it cannot work normally.

The AlTiN coating showed completely different service lives on the two substrate materials. the AlTiN coating on HSS only worked for around 100 cycles even under the smallest normal force (30 N), due to severe spalling failure. However, on the WC-Co, the service life of the AlTiN coating was improved significantly under both small and large normal forces (Figure 17c,d), due to the better bonding strength and the better deformation-resistance of WC-Co substrate. The CrN coating on HSS had dramatically longer service life and better force-resistance than the AlTiN coating on HSS. Meanwhile, the AlTiN coating on WC-Co had better force-resistance than the CrN coating on WC-Co, because the AlTiN coating had better toughness than the CrN coating. The AlTiN coating on WC-Co had poorer wear-resistance than the CrN coating on WC-Co, because the main failure mechanism of the AlTiN coating on WC-Co was abrasive and adhesive wear and CrN coating on WC-Co showed a better ability to reduce adhesive wear.

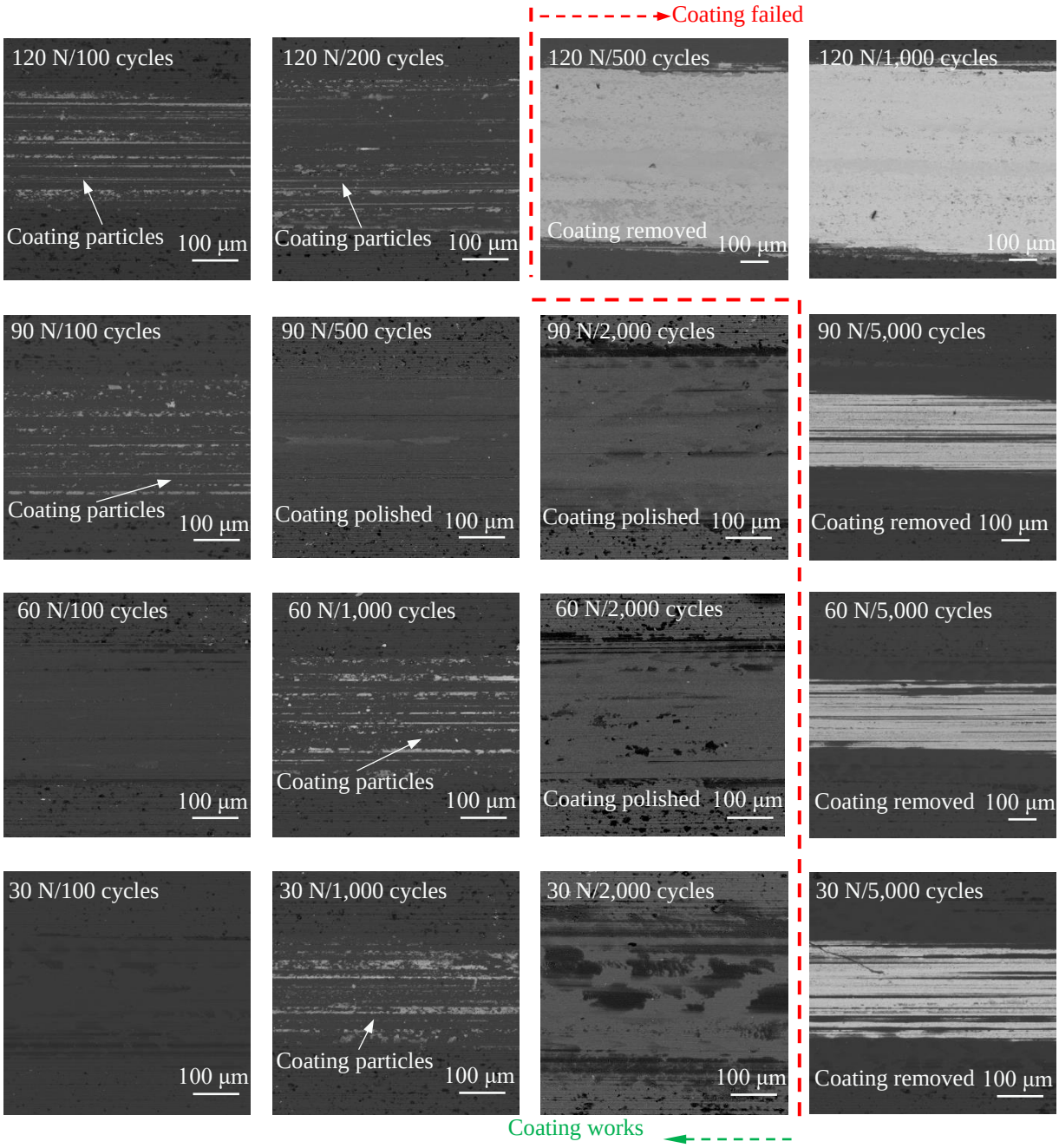

Figure 15. Wear and failure process of AlTiN coating on WC-Co substrate under different normal forces.

In summary, CrN and AlTiN were two kinds of coatings with high hardness and good wear-resistance. They were able to protect the substrate material during the process of sliding wear and reduce the damage to the substrate material. Under high normal force, CrN and AlTiN coatings would have serious spalling failure, and their service lives were low. The CrN coating had better wear-resistance than the AlTiN coating, although the AlTiN coating had higher hardness. The CrN coating had good bonding properties with both substrates due to its large grain size and chemical stability making it less prone to sticky debris. The properties of the AlTiN coating on the two substrate materials were different. The AlTiN coating on WC-Co had better force-resistance than the CrN coating on WC-Co. The AlTiN coating on WC-Co had poorer wear-resistance than the CrN coating on WC-Co.

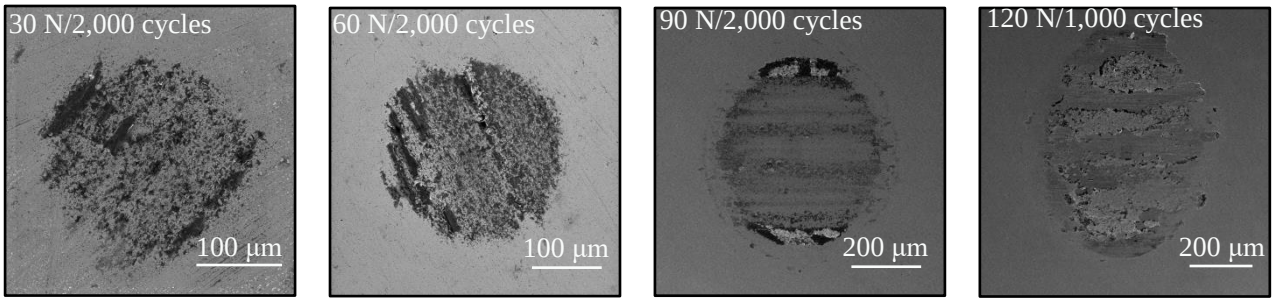

Figure 16. Wear scar of the counterbody against the AlTiN-coated WC-Co substrate under different condition.

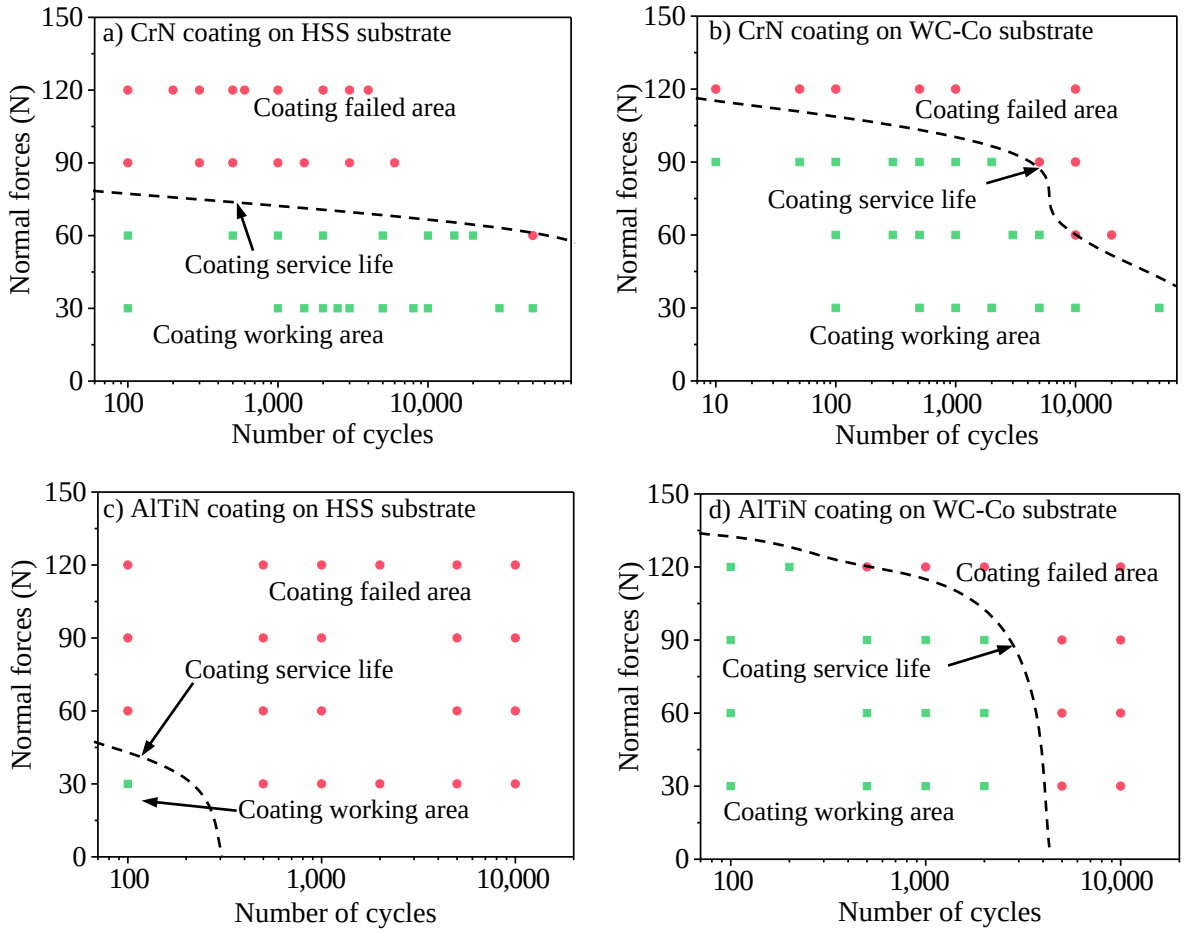

Figure 17. Coating service life maps: (**a**) CrN coating on the HSS substrate; (**b**) CrN coating on WC-Co substrate; (**c**) AlTiN coating on HSS substrate; (**d**) AlTiN coating on WC-Co substrate.

4. Conclusions

In this work, CrN and AlTiN coatings were deposited on the HSS and the WC-Co substrates. The wear processes of coatings were explored under various normal forces and after various numbers of cycles. The CoF, wear depth, wear scar morphologies during the wear process were analyzed, and the maps of the coatings service life had been constructed. The following conclusions can be drawn:

(1) The bonding strengths of the CrN and AlTiN coatings to the WC-Co substrate were larger than those to the HSS substrate. The CrN coating on WC-Co and HSS had better bonding strength than the AlTiN coating.

(2) The CoFs of HSS was in the range of 0.7–0.8 and the CoFs of WC-Co was in the range of 0.2–0.3. For the coatings (CrN and AlTiN), the CoFs were close to those of the uncoated substrates after the coatings were removed.
(3) The wear depths of uncoated HSS and WC-Co were higher than the coated ones. The wear depths were small when the coatings worked and increased with the number of cycles and normal forces. The wear depths increased obviously when the coatings were removed.
(4) For the CrN coatings under small force conditions, an adhesion layer derived from the wear debris was formed on the coating surface to reduce the wear at the beginning of the test. The main failure mechanism was abrasive wear and delamination. Under large force conditions, the main failure mechanism was spallation. For the AlTiN coatings, the main failure mechanism was spallation on the HSS substrate: however, on the WC-Co substrate it was adhesive and abrasive wear.
(5) The CrN and AlTiN coatings on WC-Co had longer service lives than on the HSS. The CrN on both substrates (HSS and WC-Co) had longer service life under smaller forces (30 N, 60 N) than AlTiN. The AlTiN coating on the HSS substrate had the smallest service life even under the smallest normal force. The CrN coating has better wear-resistance than the AlTiN coating, although the AlTiN coating has higher hardness. The service properties of the AlTiN coating on WC-Co was better than on HSS. The AlTiN coating on WC-Co had better force-resistance than the CrN coating on WC-Co. The AlTiN coating on WC-Co had poorer wear-resistance than the CrN coating on WC-Co.

Author Contributions: Writing—review and editing, supervision, Z.X.; investigation, Y.L.; resources, Z.H. All authors have read and agreed to the published version of the manuscript.

Funding: The work was supported by Key Projects of Natural Science Research in Tongling Polytechnic (tlpt2020NK006) and The Quality Engineering Project in Anhui Province (2020SJJXSFK2438).

Institutional Review Board Statement: Not applicable.

Informed Consent Statement: Not applicable.

Data Availability Statement: Not applicable.

Conflicts of Interest: The authors declare no conflict of interest.

References

1. Inspektor, P.A. Salvador, Architecture of PVD coatings for metalcutting applications: A review. *Surf. Coat. Technol.* **2014**, *257*, 138–153. [CrossRef]
2. Bouzakis, K.D.; Michailidis, N.; Skordaris, G.; Bouzakis, E.; Biermann, D.; M'Saoubi, R. Cutting with coated Tools: Coating technologies, characterization methods and performance optimization. *CIRP Ann.-Manuf. Technol.* **2012**, *61*, 703–723. [CrossRef]
3. Jadam, T.; Datta, S.; Masanta, M. Influence of cutting tool material on machinability of Inconel 718 superalloy. *Mach. Sci. Technol.* **2020**, *25*, 349–397. [CrossRef]
4. Troß, N.; Brimmers, J.; Bergs, T. Tool wear in dry gear hobbing of 20MnCr5 case-hardening steel, 42CrMo4 tempered steel and EN-GJS-700-2 cast iron. *Wear* **2021**, *476*, 203737. [CrossRef]
5. Olander, P.; Heinrichs, J. Initiation and propagation of tool wear in turning of titanium alloys -Evaluated in successive sliding wear test. *Wear* **2019**, *426–427*, 1658–1666. [CrossRef]
6. Uhlmann, E.; Hinzmann, D.; Kropidlowksi, K.; Meier, P.; Prasol, L.; Woydt, M. Substitution of commercially coated tungsten carbide tools in dry cylindrical turning process by HiPIMS coated niobium carbide cutting inserts. *Surf. Coat. Technol.* **2018**, *354*, 112–118. [CrossRef]
7. Gong, M.F.; Chen, J.; Deng, X.; Wu, S.H. Sliding wear behavior of TiAlN and AlCrN coatings on a unique cemented carbide substrate. *Int. J. Refract. Met. Hard Mater.* **2017**, *69*, 209–214. [CrossRef]
8. Kumar, T.S.; Jebaraj, A.V.; Shankar, E.; Tamiloli, N.; Sivakumar, K. Metallurgical and mechanical characterization of TiCN/TiAlN and TiAlN/TiCN bilayer nitride coatings. *Surf. Interfaces* **2019**, *15*, 256–264. [CrossRef]
9. Bobzin, K. High-performance coatings for cutting tools. *CIRP J. Manuf. Sci. Technol.* **2017**, *18*, 1–9. [CrossRef]
10. Elmkhah, H.; Mahboubi, F.; Abdollah-zadeh, A.; Rouhaghdam, A.R.S. A new approach to improve the surface properties of H13 steel for metal forming applications by applying the TiAlN multi-layer coating. *J. Manuf. Process.* **2018**, *32*, 873–877. [CrossRef]

11. Vereschaka, A.; Aksenenko, A.; Sitnikov, N.; Migranov, M.; Shevchenko, S.; Sotova, C.; Batako, A.; Andreev, N. Effect of adhesion and tribological properties of modified composite nanostructured multi-layer nitride coatings on WC-Co tools life. *Tribol. Int.* **2018**, *128*, 313–327. [CrossRef]
12. Zhou, X.K.; Wang, K.; Li, C.S.; Wang, Q.; Wu, S.; Liu, J.X. Effect of ultrafine gradient cemented carbides substrate on the performance of coating tools for titanium alloy high speed cutting. *Int. J. Refract. Met. Hard Mater.* **2019**, *84*, 105024. [CrossRef]
13. Hong, D.; Niu, Y.R.; Li, H.; Zhong, X.; Tu, W.H.; Zheng, X.B.; Sun, J.L. Comparison of microstructure and tribological properties of plasma-sprayed TiN, TiC and TiB_2 coatings. *Surf. Coat. Technol.* **2019**, *374*, 181–188. [CrossRef]
14. Xu, X.; Su, F.H.; Li, Z.J. Tribological properties of nanostructured TiAlN/W_2N multilayer coating produced by PVD. *Wear* **2019**, *430–431*, 67–75. [CrossRef]
15. Chen, Y.J.; Wang, S.H.; Hao, Y.; Pu, J.B.; Jiang, X.; Huang, L.F.; Wang, L.P. Friction and Wear Behavior of CrN Coating on 316L Stainless Steel in Liquid Sodium at Elevated Temperature. *Tribol. Int.* **2020**, *143*, 106079. [CrossRef]
16. Zhang, W.H.; Hsieh, J.H. Tribological behavior of TiN and CrN coatings sliding against an epoxy molding compound. *Surf. Coat. Technol.* **2000**, *130*, 240–247. [CrossRef]
17. Ding, X.Z.; Zeng, X.T.; Liu, Y.C.; Fang, F.Z.; Lim, G.C. $Cr_{1-x}Al_xN$ coatings deposited by lateral rotating cathode arc for high speed machining applications. *Thin Solid Film.* **2008**, *516*, 1710–1715. [CrossRef]
18. Mei, F.S.; Chen, Y.; Zhang, H.D.; Lin, X.L.; Gao, J.X.; Yuan, T.H.; Cao, X.X. Greater improvement of carbon and boron co-doping on the mechanical properties, wear-resistance and cutting performance of AlTiN coating than that of doping alone. *Surf. Coat. Technol.* **2021**, *406*, 126738. [CrossRef]
19. Mo, J.L.; Zhu, M.H. Sliding tribological behaviors of PVD CrN and AlCrN coatings against Si3N4 ceramic and pure titanium. *Wear* **2009**, *267*, 874–881. [CrossRef]
20. Zhou, F.; Suh, C.M.; Kim, S.S. Ri-ichi Murakami, Sliding-wear behavior of TiN- and CrN-coated 2024 aluminum alloy against an Al_2O_3 ball. *Tribol. Lett.* **2002**, *13*, 173–178. [CrossRef]
21. Birol, Y. Sliding wear of CrN, AlCrN and AlTiN coated AISI H13 hot work tool steels in aluminium extrusion. *Tribol. Int.* **2013**, *57*, 101–106. [CrossRef]
22. Tillmann, W.; Grisales, D.; Stangier, D. Effects of AISI H11 surface integrity on the residual stresses and adhesion of TiAlN/substrate compounds. *Surf. Coat. Technol.* **2019**, *357*, 466–472. [CrossRef]
23. Geng, Z.; Shi, G.L.; Shao, T.M.; Liu, Y.; Duan, D.L.; Reddyhof, T. Tribological behavior of patterned TiAlN coatings at elevated temperatures. *Surf. Coat. Technol.* **2019**, *364*, 99–114. [CrossRef]
24. Madah, F.; Dehghanian, C.; Amadeh, A.A. Investigations on the wear mechanisms of electroless Ni–B coating during dry sliding and endurance life of the worn surfaces. *Surf. Coat. Technol.* **2015**, *282*, 6–15. [CrossRef]
25. Wang, Q.Q.; Jin, Z.J.; Zhao, Y.; Niu, L.; Guo, J. A comparative study on tool life and wear of uncoated and coated cutting tools in turning of tungsten heavy alloys. *Wear* **2021**, *482–483*, 203929. [CrossRef]
26. Zhao, J.F.; Liu, Z.Q.; Wang, B.; Hu, J.R.; Wan, Y. Tool coating effects on cutting temperature during metal cutting processes: Comprehensive review and future research directions. *Mech. Syst. Sign. Process.* **2021**, *150*, 107302. [CrossRef]
27. Tebaldo, V.; Kilpi, L.; Ronkainen, H.; Faga, M.G. Tribological properties of AlTIN coating in sliding contact with Ti6Al4V: A helpful tool for disentangling the phenomena complexity during real turning operations. *Tribol. Int.* **2018**, *123*, 71–80. [CrossRef]
28. Zhang, Q.; Xu, Y.X.; Zhang, T.F. Tribological properties, oxidation resistance and turning performance of AlTiN/AlCrSiN multilayer coatings by arc ion plating. *Surf. Coat. Technol.* **2018**, *356*, 1–10. [CrossRef]
29. Zheng, G.M.; Zhao, G.Y.; Cheng, X.; Xu, R.F.; Zhao, J.; Zhang, H.Q. Frictional and wear performance of TiAlN/TiN coated tool against high strength steel. *Ceram. Int.* **2018**, *44*, 6878–6885. [CrossRef]
30. Heinrichs, J.; Mikado, H.; Wiklund, U.; Jacobson, S. Wear of uncoated and PVD coated cemented carbide tools for processing of copper based materials part II: Exploring the sliding contact with pure copper. *Wear* **2021**, *466–467*, 203589. [CrossRef]
31. Azhaarudeen, S.; Faruck, A.A.M.; Nevosad, A. Tribological behaviour and wear mechanisms of manganese phosphate coatings under dry reciprocating sliding contact conditions. *Tribol. Int.* **2018**, *122*, 189–199. [CrossRef]
32. Vera, E.E.; Vite, M.; Lewis, R.; Gallardo, E.A.; Laguna-Camacho, J.R. A study of the wear performance of TiN, CrN and WC/C coatings on different steel substrates. *Wear* **2011**, *271*, 2116–2124. [CrossRef]
33. Xian, G.; Xiong, J.; Zhao, H.B.; Fan, H.Y.; Li, Z.X.; Du, H. Evaluation of the structure and properties of the hard TiAlN-(TiAlN/CrAlSiN)-TiAlN multiple coatings deposited on diverse substrate materials. *Int. J. Refract. Met. Hard Mater.* **2019**, *85*, 105056. [CrossRef]
34. Łępicka, M.; Grądzka-Dahlke, M.; Pieniak, D.; Pasierbiewicz, K.; Kryńska, K.; Niewczas, A. Tribological performance of titanium nitride coatings: A comparative study on TiN-coated stainless steel and titanium alloy. *Wear* **2019**, *422–423*, 68–80. [CrossRef]
35. Zhou, Y.F.; Ma, W.D.; Geng, J.; Wang, Q.; Rao, L.X.; Qian, Z.Y.; Xing, X.L.; Yang, Q.X. Exploring long-run reciprocating Wear of diamond-like carbon coatings: Microstructural, morphological and tribological evolution. *Surf. Coat. Technol.* **2021**, *405*, 126581. [CrossRef]
36. Ding, H.H.; Fridrici, V.; Geringer, J.; Fontaine, J.; Kapsa, P. Influence of diamond-like carbon coatings and roughness on fretting behaviors of Ti-6Al-4V for neck adapter-femoral stem contact. *Wear* **2018**, *406–407*, 53–67. [CrossRef]
37. Ding, H.H.; Fridrici, V.; Bouvard, G.; Geringer, J.; Fontaine, J.; Kapsa, P. Influence of Deposition Positions on Fretting Behaviors of DLC Coating on Ti-6Al-4V. *Tribol. Trans.* **2019**, *62*, 1155–1172. [CrossRef]

38. Ding, H.H.; Fridrici, V.; Bouvard, G.; Geringer, J.; Kapsa, P. Influence of Calf Serum on Fretting Behaviors of Ti-6Al-4V and Diamond-Like Carbon Coating for Neck Adapter–Femoral Stem Contact. *Tribol. Lett.* **2018**, *66*, 110. [CrossRef]
39. León-Patiño, C.A.; Braulio-Sánchez, M.; Aguilar-Reyes, E.A.; Bedolla-Becerril, E.; Bedolla-Jacuinde, A. Dry sliding wear behavior of infiltrated particulate reinforced Ni/TiC composites. *Wear* **2019**, *426–427*, 989–995. [CrossRef]
40. Mo, J.L.; Zhu, M.H.; Leyland, A.; Matthews, A. Impact wear and abrasion resistance of CrN, AlCrN and AlTiN PVD coatings. *Surf. Coat. Technol.* **2013**, *215*, 170–177. [CrossRef]
41. Zhang, K.; Deng, J.; Guo, X.; Sun, L.; Lei, S. Study on the adhesion and tribological behavior of PVD TiAlN coatings with a multi-scale textured substrate surface. *Int. J. Refract. Met. Hard Mater.* **2018**, *72*, 292–305. [CrossRef]
42. De Oliveira Junior, M.M.; Costa, H.L.; Junior, W.M.S.; de Mello, J.D.B. Effect of iron oxide debris on the reciprocating sliding wear of tool steels. *Wear* **2019**, *426–427*, 1065–1075. [CrossRef]